*chips*

MDPI

*Article*

# Enhanced Adhesion Strength of Copper/Epoxy Composite Build-Up Films for Flip-Chip Ball Grid Array Substrates via Interfacial Chemical Modification

**Shanjun Ding [1,*], Xiaowen Lin [1,2], Mengxi Liu [1], Man Li [1], Qichang An [1,3], Chuan Chen [1], Xiaomeng Wu [1,3], Zhidan Fang [1] and Qidong Wang [1,*]**

[1] Institute of Microelectronics of the Chinese Academy of Sciences, Beijing 100029, China; linxiaowen25@mails.ucas.ac.cn (X.L.); liumengxi@ime.ac.cn (M.L.); liman2025@ime.ac.cn (M.L.); anqichang@ime.ac.cn (Q.A.); chenchuan@ime.ac.cn (C.C.); wuxiaomeng@ime.ac.cn (X.W.); fangzhidan@ime.ac.cn (Z.F.)
[2] School of Integrated Circuits, University of Chinese Academy of Sciences, Beijing 100029, China
[3] Key Laboratory of Fabrication Technologies for Integrated Circuits, Institute of Microelectronics of the Chinese Academy of Sciences, Beijing 100029, China
* Correspondence: shanjunding@gmail.com (S.D.); wangqidong@ime.ac.cn (Q.W.)

**Abstract**

The interfacial adhesion strength of fine lines for flip-chip ball grid array (FCBGA) substrates is highly dependent on the surface desmear process during substrate manufacturing. However, the extremely narrow window for optimal desmear processes limits the improvement of the adhesion strength of fine lines. Herein, a polydopamine-modified epoxy build-up film substrate was fabricated to increase chemical bonding action and broaden the process window. The chemical structure, surface roughness, morphology, surface chemical state, and adhesion strength of the modified substrate were characterized. The results showed that the adhesion strength of the substrates increased from 2.2 N/cm to 4.1 N/cm under suboptimal process conditions. Meanwhile, the effect of the polydopamine deposition time on the adhesion strength of the copper-deposited epoxy resin composite films at the interfaces was systematically investigated; furthermore, the mechanisms and reasons for the increased adhesion strength and interfacial adhesion failure for the copper-deposited epoxy resin composite build-up film substrates were revealed. This work will provide guidance in both theory and experiment to enhance the interfacial adhesion force for advanced substrates in the future.

**Keywords:** advanced packaging; FCBGA substrate; surface modification; adhesion strength

Check for updates

Academic Editor: Lung-Chien Chen

Received: 15 June 2026
Revised: 19 July 2026
Accepted: 27 July 2026
Published: 4 August 2026

**Copyright:** © 2026 by the authors. Licensee MDPI, Basel, Switzerland. This article is an open access article distributed under the terms and conditions of the Creative Commons Attribution (CC BY) license.

## 1. Introduction

Flip-chip ball grid array (FCBGA) substrates have been widely used as a core carrier for chiplet-scale integration driven by artificial intelligence (AI), graphics processing units (GPUs), and central processing units (CPUs) because they can provide higher interconnect density and larger form factors [1–3]. To further improve the interconnect density of the substrate, the line width and line spacing (L/S) of fine lines are being aggressively reduced from 15 μm to 2 μm, while the substrate size is expanding from 80 mm × 80 mm in 2023 to an expected 120 mm × 150 mm by 2027 [4]. However, the interfacial adhesion strength between the copper lines and the epoxy composite film degrades significantly due to the low surface roughness of the epoxy composite film, which severely limits further improvements in the adhesion strength of fine lines. Meanwhile, determining the optimal

process parameters to enhance interfacial adhesion strength within an extremely narrow surface-roughening process window presents significant challenges, including lengthy process exploration and issues related to process stability [5,6]. Therefore, effectively addressing the instability of surface chemical roughening process parameters and broadening the narrow process window are highly desired in the industry.

To address this issue, researchers have primarily adopted two strategies: the first focuses on optimizing process parameters using traditional surface chemical roughening techniques, whereas the second involves the chemical modification of roughened Ajinomoto build-up film (ABF) surfaces using functional groups. Regarding the first strategy, for instance, Kempa et al. [7] introduced a newly developed alkaline cleaner process with a specially designed surfactant system to remove $SiO_2$ fillers from the surface of ABF resins, thereby increasing surface roughness. As a result, the peel strength was significantly increased to 4 N/cm. Murayama et al. [8] modified the ABF surface using oxygen radicals generated by $O_2$ plasma, followed by the deposition of copper onto the modified ABF; consequently, the adhesion strength of the Cu/ABF interface increased from 2.7 to 3.8 N/cm. Recently, our group [9] also investigated the effect of swelling time on the adhesion strength between copper and the epoxy composite film for the substrate. When the swelling time was increased from 5 to 30 min, the adhesion strength rose from 3.4 to 4.8 N/cm. Although the aforementioned methods can effectively enhance the adhesion strength of substrates, these results remain highly dependent on the stability of the chemical properties required for surface roughening and strict process control conditions. To overcome this challenge, the chemical properties of the epoxy composite film surface must be maintained stably. Regarding the second strategy, specific chemical groups are introduced to modify the roughened ABF surface. For instance, Wang et al. [10] utilized sodium thiosulfate to modify the surface of epoxy resins to enhance the adhesion strength between Ag and the resin. Their results demonstrated an adhesion grade of 5B, which was attributed to the enhanced interfacial chemical bonding strength provided by the thiosulfate groups. However, despite its capability to improve interfacial adhesion strength, sodium thiosulfate exhibits relatively poor thermal stability and tends to decompose at elevated temperatures. Consequently, its application in actual high-temperature substrate curing processes remains difficult. To resolve this limitation, polydopamine (PDA) is used to increase adhesion strength between $SiO_2$ and copper as well as epoxy resin and copper foil [11–13]. For instance, Zhu et al. [12] used silane and PDA to prepare a silane coating with PDA coating on the surface of copper foil by electrodeposition. The peel strength is increased by about 42.15%. This work can increase peel strength between epoxy resin and copper foil, but it is also unsuitable for packaging substrates because silane-PDA coatings are difficult to deposit on ABF substrate surfaces. Furthermore, the limited number of polar groups such as hydroxyl groups remaining on the ABF surface after oxidation hinders subsequent electroless copper plating. Additionally, silane deposition increases the process stability of the ABF substrate, making this approach unsuitable for packaging substrate manufacturing. Therefore, directly depositing PDA onto the ABF surface to improve interfacial adhesion is quite attractive. Schaubroeck et al. [13] employed certain polyamines and PDA to modify epoxy resin surfaces and studied the resulting impacts on interfacial adhesion strength. Their findings indicated that the adhesion strength reached over 6 N/cm at a surface roughness of Ra $\geq$ 600 nm. However, although this interfacial chemical bonding compensates for the adhesion loss, such modifications remain highly dependent on high surface roughness, making it challenging to meet the concurrent requirements of low roughness and high adhesion. Based on the current literature, achieving high interfacial adhesion on ABF surfaces with low surface roughness through chemical modification remains an unresolved challenge.

Polydopamine (PDA) is a mussel-inspired polymer capable of forming strong chemical and physical bonds with numerous inorganic, metallic, and organic materials [14,15]. It primarily achieves robust adhesion through the polar functional groups in its molecular structure, such as amine, quinone, phenolic hydroxyl, and indole groups. Furthermore, dopamine can readily self-polymerize at room temperature, and this polymerization behavior can be precisely controlled by adjusting reaction conditions, making PDA an ideal surface chemical modifier. In addition, PDA deposited on Ajinomoto build-up film (ABF) surfaces can enhance interfacial adhesion strength by regulating the evolution of interfacial copper oxides through its abundant polar chemical groups. Besides enhancing interfacial adhesion, PDAs also need to accommodate the high-temperature processes of the packaging substrate, such as reflow. While the initial thermal decomposition temperature of PDAs in air or oxygen-containing environments is approximately 200–220 °C [16,17], according to relevant literature, the initial thermal decomposition temperature of PDAs in inert or sealed environments can reach over 270 °C, even 340 °C [18,19]. Therefore, the integration of PDAs into the packaging substrate demonstrates significant potential for compatibility with the substrate's high-temperature processes, such as reflow. Simultaneously, due to the high cross-linking density formed by PDA polymerization, it exhibits good resistance to acidic and alkaline solutions in wet chemical processes and metallization to some extent [20]. Therefore, PDAs can adapt well to packaging substrate processing technologies.

In this work, dopamine was utilized to modify the surface of the roughened epoxy resin composite build-up film. Subsequently, the PDA layer and copper were deposited sequentially onto the ABF surface via self-polymerization and electroless copper plating to fabricate Cu/ABF structures for large-sized chip substrates. The effects of PDA on the interfacial copper oxides and the overall adhesion strength were systematically investigated. The chemical structure, surface roughness, morphology, surface chemical states, and adhesion strength between the copper and the epoxy resin substrate were fully characterized. Moreover, the influence of the PDA deposition time on the evolution of copper oxides and the underlying mechanisms was revealed in detail. To the best of our knowledge, studies focusing on the regulation of surface roughness and copper oxidation state tuned by PDA deposition conditions to optimize the adhesion properties of FCBGA substrates remain highly scarce so far.

## 2. Materials and Methods

### *2.1. Materials*

Epoxy resin composite film with 72 wt.%$SiO_2$ (ABF) is supplied by Ajinomoto Fine-Techno Co., Inc., Japan. with applications in the microelectronics industry. Core board with a thickness of 0.8 mm is supplied by Guangdong Shengyi Technology Co., Ltd., China. Dopamine hydrochloride, copper sulfate, hydrogen peroxide, and hydrochloric acid buffer with pH = 8.5 are purchased from Aladdin, China. All reagents are not further processed.

### *2.2. Preparation of ABF Substrates*

The epoxy composite films were hot-pressed onto the surface of a core board at 0.7 MPa and 100 °C, followed by a two-stage curing process of the ABF substrate at 120 °C for 30 min and 180 °C for 30 min. After curing, the surface of the ABF was first roughened via swelling (70 °C for 30 min) and desmearing (80 °C for 20 min) processes. Subsequently, the ABF substrate was cut into 10 cm × 10 cm samples using a milling machine. The overall fabrication process of the PDA@ABF substrates is schematically illustrated in Figure 1.

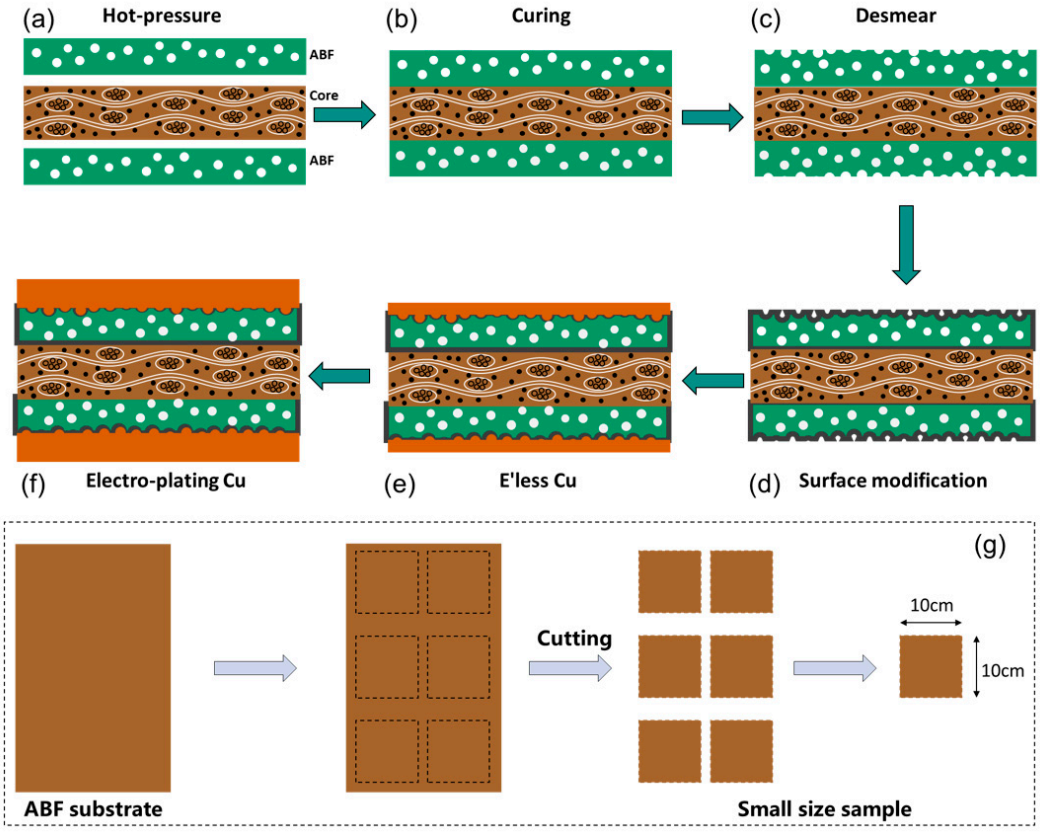


**Figure 1.** Schematic diagram of the whole preparation process for ABF surface metallization: (**a**) hot-pressure; (**b**) curing; (**c**) desmear; (**d**) surface modification; (**e**) E'less; (**f**) Electro-plating Cu; (**g**) Schematic diagram of panel-level substrate cutting.

### *2.3. Preparation of PDA@ABF Substrates*

A dopamine hydrochloride solution (2 mg/mL, 1000 mL) was prepared in a hydrochloric acid buffer solution containing copper sulfate and hydrogen peroxide, with a molar ratio of copper sulfate to hydrogen peroxide maintained at 1:2. Subsequently, the square samples were immersed in the 1000 mL dopamine hydrochloride solution at room temperature for various deposition times (0, 2, 5, and 10 min), and polymerization mechanism of polydopamine is shown in Figure S1. The resulting PDA@ABF substrates were first rinsed with deionized water and then dried at 80 °C for 60 min to enhance the chemical crosslinking density of the polydopamine on the ABF surface. Following this surface modification, a copper layer was deposited onto the roughened PDA@ABF surface via sequential electroless copper plating and electroplating to achieve complete surface metallization. Finally, the metalized samples were annealed at 190 °C for 60 min, as shown in Figure 2.

### *2.4. Characterization*

The molecular structure is tested by a Fourier Transform Infrared Spectroscopy-Attenuated Total Reflectance (FTIR-ATR, Perkin Elmer Spectrum TM 100 FTIR, United States); Surface morphology of ABF substrates is characterized by scanning electron microscope (SEM, HITACHI STA200, Japan and ZEISS Sigma 360, Germany); The surface roughness of substrates was characterized by an interference microscope MIC-250 (ATOS GmbH, Germany); The chemical state is examined using an X-ray photoelectron spectroscopy (XPS, Thermo Scientific K-Alpha, United States) fitted with an Al K$\alpha$ radiation source (1486.6 eV); Peel strength of ABF substrates is tested by Universal testing machine (AG-X Plus, Shimadzu, Japan) at room temperature with a crosshead speed of 50 mm/min.

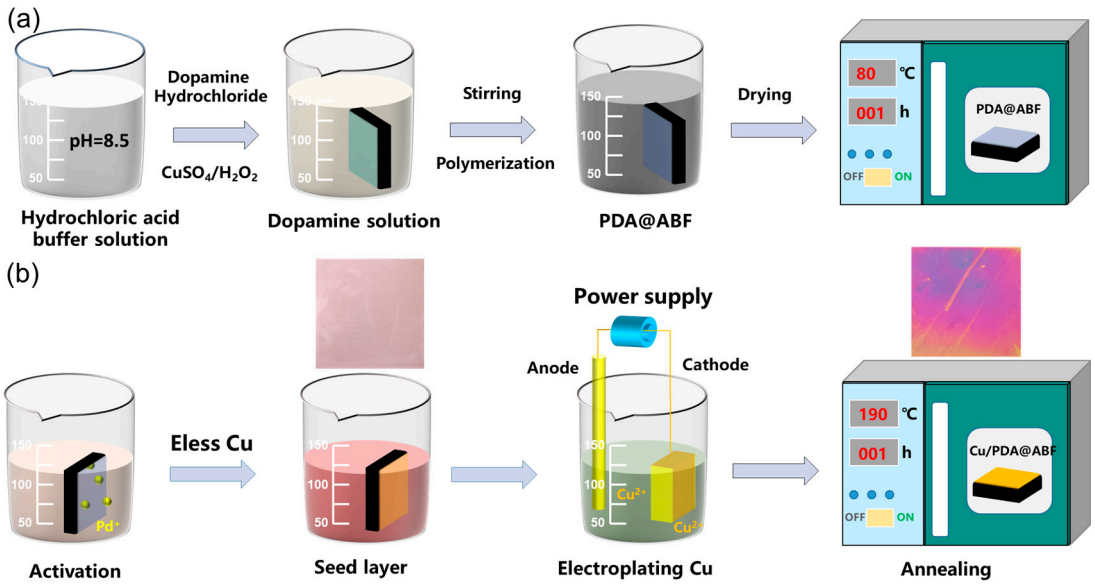


**Figure 2.** Schematic diagram of (**a**) PDA modified ABF substrates, (**b**) their surface metallization.

## 3. Results and Discussion

To characterize the dopamine-mediated surface modification on the ABF substrates, the FT-IR spectra of the pristine ABF and PDA@ABF substrates are shown in Figure 3a. As observed, the characteristic peaks of both the ABF and PDA@ABF substrates appear at the same positions; however, the peak intensities for the PDA@ABF substrate are noticeably higher than those of the pristine ABF substrate. This phenomenon can be primarily attributed to two factors: first, the chemical functional groups in both ABF and PDA (such as C–C, C–N, and C–O bonds) are identical, and the presence of the PDA layer mutually reinforces the intensity of these FT-IR spectral peaks; second, the surface color of the PDA@ABF substrate becomes darker in comparison with that of the pristine ABF surface, as depicted in the optical inset of Figure 3a. Therefore, these spectroscopic results confirm that PDA was successfully deposited onto the ABF surface. Furthermore, Figure 3b shows the XPS survey spectra of the ABF and PDA@ABF substrates. Three distinct peaks located at approximately 285, 400, and 532 eV can be clearly observed, corresponding to the C 1s, N 1s, and O 1s photoelectrons in both samples. Upon modification of the ABF surface with PDA, the N/C and N/O atomic ratios increased significantly. This trend further indicates the successful deposition of PDA onto the ABF substrate, which is ascribed to the abundant amine groups within the PDA structure that inherently enhance the intensity of the N 1s peak. In addition, the surface morphologies of the ABF and PDA@ABF samples were characterized by SEM, as shown in Figure 3c,d. Visually, the surface topographies of the two ABF samples before and after PDA modification are highly similar, demonstrating that the PDA modification does not alter the surface roughness or morphology of the ABF during substrate manufacturing. Consequently, the aforementioned characterizations collectively indicate that dopamine formed a uniform and functionalized conformal coating on the ABF surface via oxidative self-polymerization.

To analyze the effect of PDA deposition on the interfacial adhesion mechanism between the copper and the ABF, the surface topographies of the peeled ABF substrates under different PDA deposition times were characterized, as shown in Figure 4. Clear spherical silica particles and the corresponding pits left after their detachment can be observed on all peeled ABF surfaces, which contrasts with the SEM morphologies of the as-desmeared ABFs (see Figure 4c,d). This indicates that the interfacial fracture primarily initiated at the physical interface between the resin and the copper layers. As the PDA deposition

time on the ABF surface increased, the topographies of the peeled substrates exhibited no prominent differences, all retaining a large number of exposed fillers and resin matrix. These highly roughened failure surfaces indicate that a robust mechanical interlocking force had been established between the copper and the ABF substrate. Furthermore, the elemental compositions of the peeled ABF substrates were analyzed via energy-dispersive spectroscopy (EDS) to investigate the distribution of characteristic elements, as shown in Figure 5. While the distributions of carbon, oxygen, copper, and silicon were clearly observable on the ABF surfaces, nitrogen remained undetected, which is primarily attributed to its trace content within the bulk resin and the ultra-thin PDA layer. According to the EDS quantitative results in Figure 5, the residual copper contents on the peeled ABF surfaces with different PDA deposition times (0, 2, 5, and 10 min) were 0.83 wt.%, 3.00 wt.%, 1.74 wt.%, and 3.06 wt.%, respectively. The residual copper content on the pristine ABF substrate (0 min) was significantly lower than that on the PDA-modified substrates, confirming that the interfacial chemical bonding between the copper and the unmodified ABF was extremely weak. Upon PDA modification, the interfacial chemical bonding was substantially enhanced; consequently, more copper cohesive failure occurred, leaving higher amounts of residual copper on the ABF surface after peeling. Specifically, at a PDA deposition time of 5 min, where the adhesion strength reached its peak, the enhanced interfacial bonding forced the fracture path to partially shift into the copper layer, thereby yielding the lowest residual copper content on the peeled ABF surface. However, when the PDA deposition time was further extended to 10 min, the excessive accumulation of PDA aggregates might instead form a weak boundary layer or hinder the effective coordination/diffusion of copper ions into the active sites of the modified film, resulting in a slight degradation of adhesion strength and a corresponding decrease in residual copper content to 3.06 wt.%.

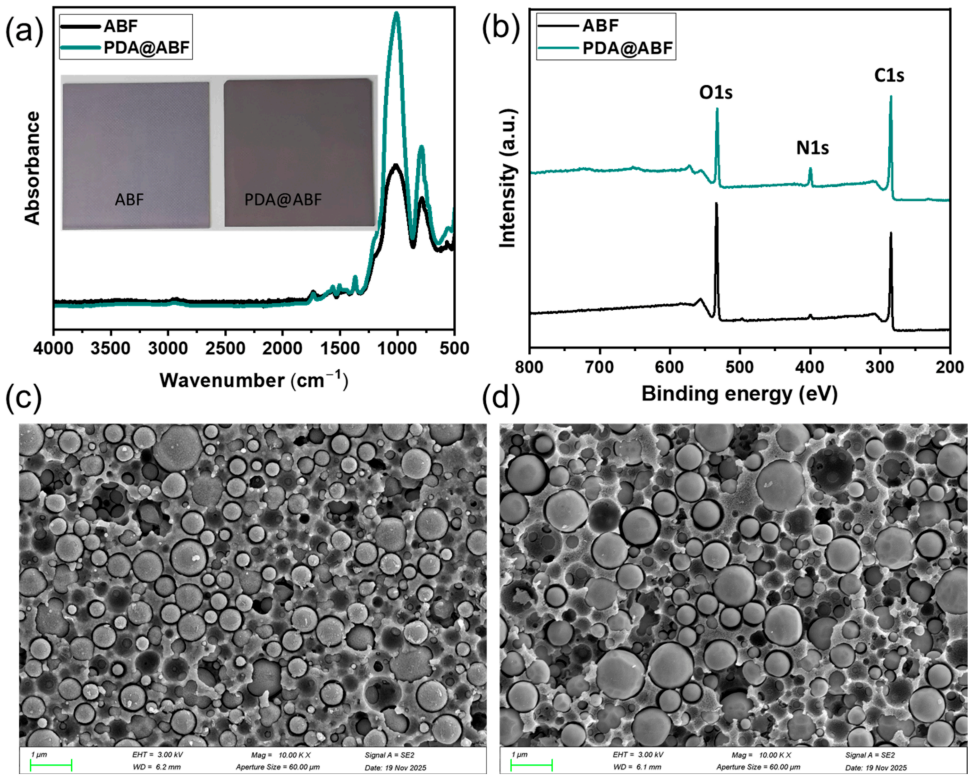


**Figure 3.** Microstructure characterizations of ABF and PDA@ABF substrates: (**a**) FT-IR spectrum; (**b**) XPS survey spectrum; SEM morphology (**c**) before modification and (**d**) after modification.

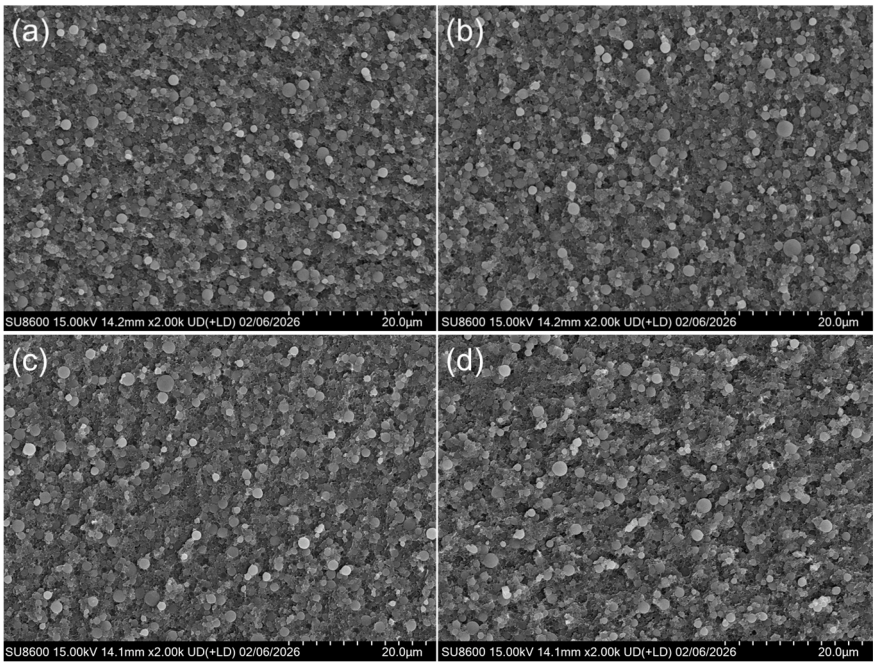


**Figure 4.** SEM morphologies of peeled ABF substrates with different deposition times: (**a**) 0 min, (**b**) 2 min, (**c**) 5 min, and (**d**) 10 min.

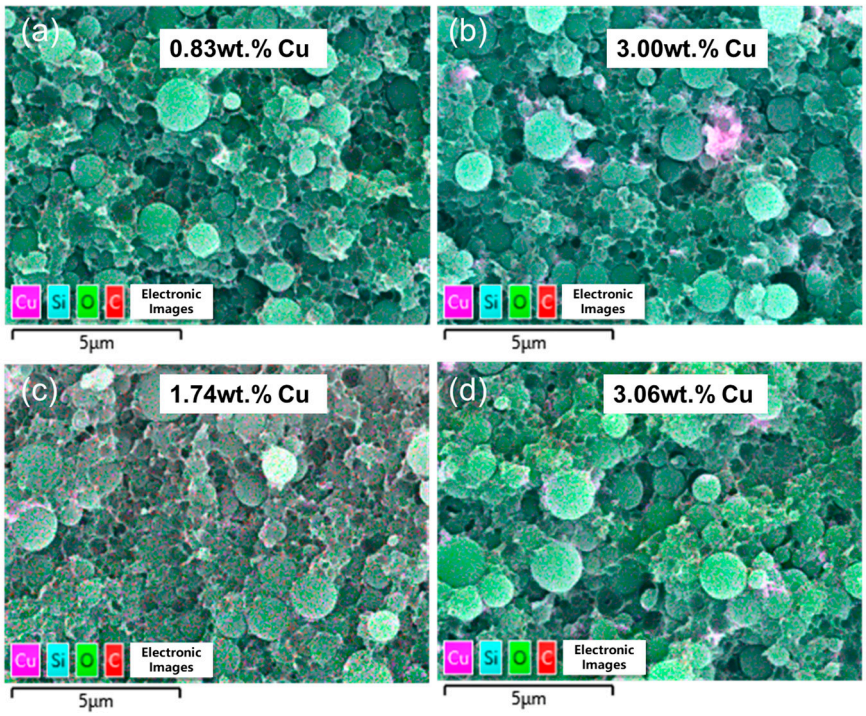


**Figure 5.** Surface EDS of peeled ABF substrates with different deposition times: (**a**) 0 min, (**b**) 2 min, (**c**) 5 min, and (**d**) 10 min.

In order to further analyze the surface structure of the peeled ABF substrates, the surface roughness of the peeled ABF with different deposition times was characterized, as shown in Figure 6. When the PDA deposition time increased from 0 min to 10 min, the surface roughness Ra of the peeled ABF substrates was 290, 364, 360, and 364 nm, respectively. These results indicate that the introduction of PDA deposition at the interfaces can increase the surface roughness in comparison with the initial ABF substrate, implying that introducing PDA enhances the interfacial adhesion strength because PDA can increase

the interfacial chemical bonding action. At the same time, the extension of the PDA deposition time does not have an obvious influence on the surface roughness of the peeled ABF substrates, which is mainly attributed to the following factors: one is that more torn resin and PDA residues remain on the ABF peel surface; the other is that the different interfacial adhesion strengths can form a fracture morphology with the same cycle.

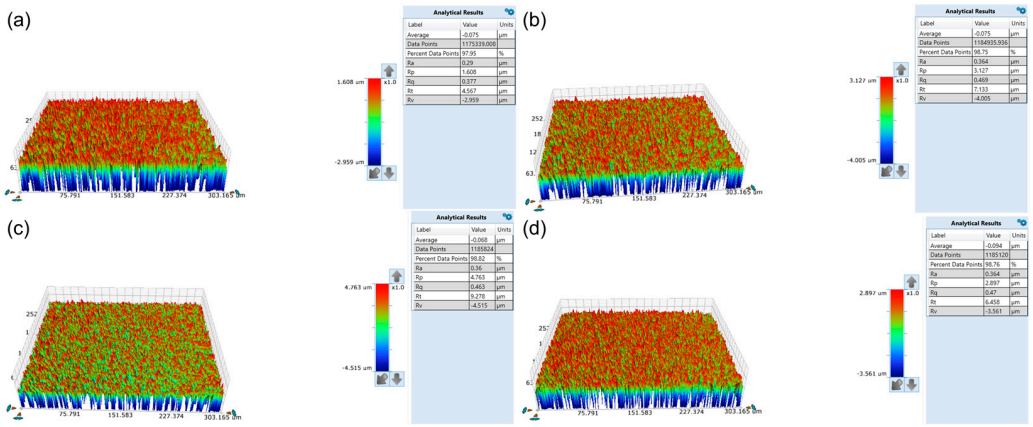


**Figure 6.** Surface roughness of peeled ABF substrates with different deposition times: (**a**) 0 min, (**b**) 2 min, (**c**) 5 min, and (**d**) 10 min.

Meanwhile, the surface morphologies of the peeled copper strips after PDA deposition with different times were also characterized by SEM, as shown in Figure 7. As seen, numerous fillers and pits, as well as resin, exist on the surface of the peeled copper strips. The above results are attributed to the following factors: one is that copper atoms deposited into the gaps between silicon oxide and epoxy resin, and then the silicon oxide fillers were coated with copper to form a mechanical anchoring effect; the other is that the ABF surface possesses polar groups such as hydroxyl, amino, and phenolic hydroxyl groups, as well as indole structures, after the PDA surface chemical modification, and these groups form C-O-Cu and C-N-Cu chemical bonds and hydrogen bonds with copper oxide at the interfaces. Meanwhile, there are slight differences in the surface morphologies of all the peeled copper strips. For instance, the initial peeled copper strip surface has obvious and clear filler pits, while other peeled copper strip surfaces exhibit some resin tears, resulting in unclear filler pits. As shown in Figure 8, the EDS results show the distributions of carbon, oxygen, copper, and silicon on the surface of the peeled copper strips, indicating that the interfacial fracture mainly occurs inside the resin. At the same time, the change trends of copper content on the surface of the peeled copper strips and the peeled ABF substrates are consistent.

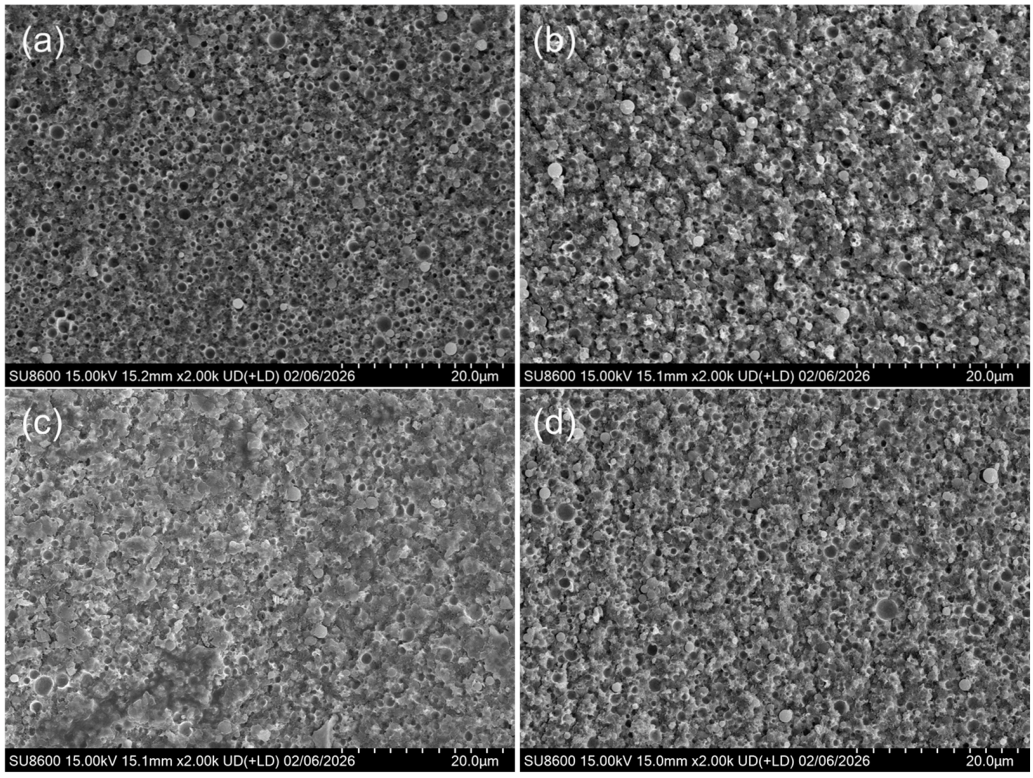


**Figure 7.** SEM morphologies of peeled copper strips with different deposition times: (**a**) 0 min, (**b**) 2 min, (**c**) 5 min, and (**d**) 10 min.

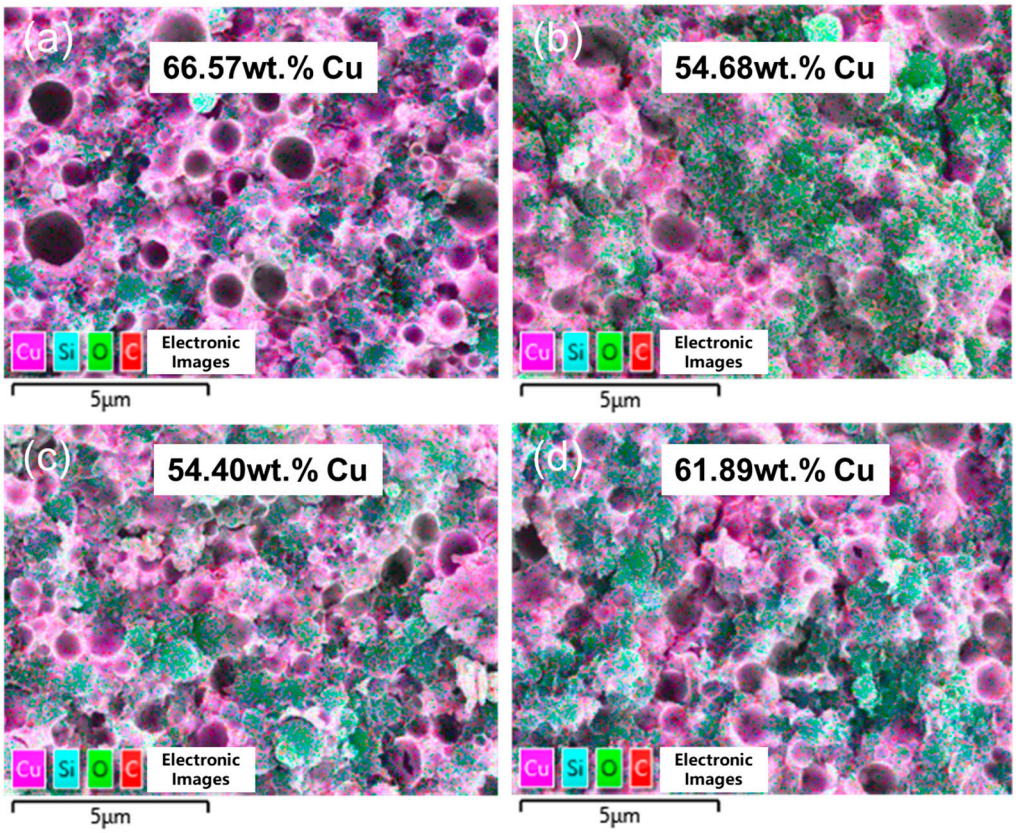


**Figure 8.** Surface EDS of peeled copper strips with different deposition times: (**a**) 0 min, (**b**) 2 min, (**c**) 5 min, and (**d**) 10 min.

The interfacial adhesion strength is related to the chemical bonding behavior between the copper and the substrate [21,22]. As far as we know, some copper oxides will be generated at the interfaces during the electroless copper plating process, and these copper oxides can react with some polar groups from the resin substrates after the wet desmear process to form chemical covalent bonds [23,24]. X-ray photoelectron spectroscopy (XPS) is an effective method for studying interfacial chemical bonding. Figure S3 shows the XPS survey spectra of the peeled copper strip surfaces with different PDA deposition times. As seen, some characteristic chemical element peaks are observed, which correspond to Si 2p, C 1s, N 1s, O 1s, Cu LMM, and Cu 2p, respectively. In order to deeply analyze the characteristic chemical states, the C 1s, N 1s, O 1s, Cu 2p, and Cu LMM peaks of the peeled copper strips with different PDA deposition times were studied sequentially. Figure 9 shows the C 1s XPS spectra of the peeled copper strips with different deposition times. These peaks were first fitted using Origin software version 9.0 and subsequently deconvoluted into three peaks, which are assigned to the C-C, C-O, and C=O bonds of the molecular chains. The fitted results are summarized in Table S1. With the increase in PDA deposition times, the integral area of the C-C bond gradually increased from 79.28% to 80.96%, indicating that more resin molecular chains remained on the copper strip surfaces after peeling. At the same time, the total integral area of the C=O bond first increases and then decreases. This result is attributed to the fact that PDA can enhance the interfacial chemical bonding action because the C=O groups in the PDA molecular structure can react with copper and its oxides, while an excessive PDA content will decrease the adhesion action due to the weak cohesive energy in PDA.

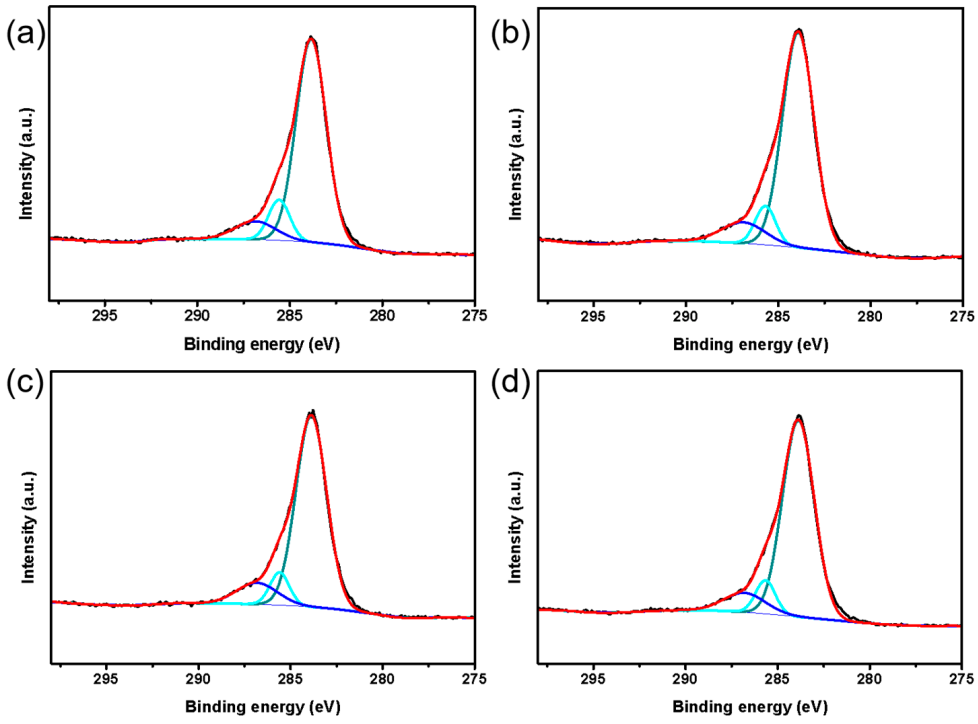


**Figure 9.** C 1s XPS spectra of peeled ABF substrates with different deposition times: (**a**) 0 min; (**b**) 2 min; (**c**) 5 min; (**d**) 10 min.

The O 1s XPS spectra of the peeled copper strips with different PDA deposition times are shown in Figure 10. All the peaks were fitted using Origin software version 9.0, and all the O 1s peaks were deconvoluted into three peaks that are assigned to C-O, C=O, and Cu-O bonds. The C=O and C-O peaks are mainly sourced from the ABF and PDA molecular chains, while the Cu-O peak is primarily attributed to the copper oxides at the

interface. The fitted integral area results of all the O 1s peaks are listed in Table S2. As the PDA deposition time increased from 0 to 10 min, the total integral area of the Cu-O peak first decreased from 14.05% to 9.32% and then increased to 10.31%. This trend indicates that the introduction of PDA can regulate the evolution of copper oxides, because the abundant polar groups in PDA can form chemical bonds with cuprous oxide and copper, thereby inhibiting further copper oxidation.

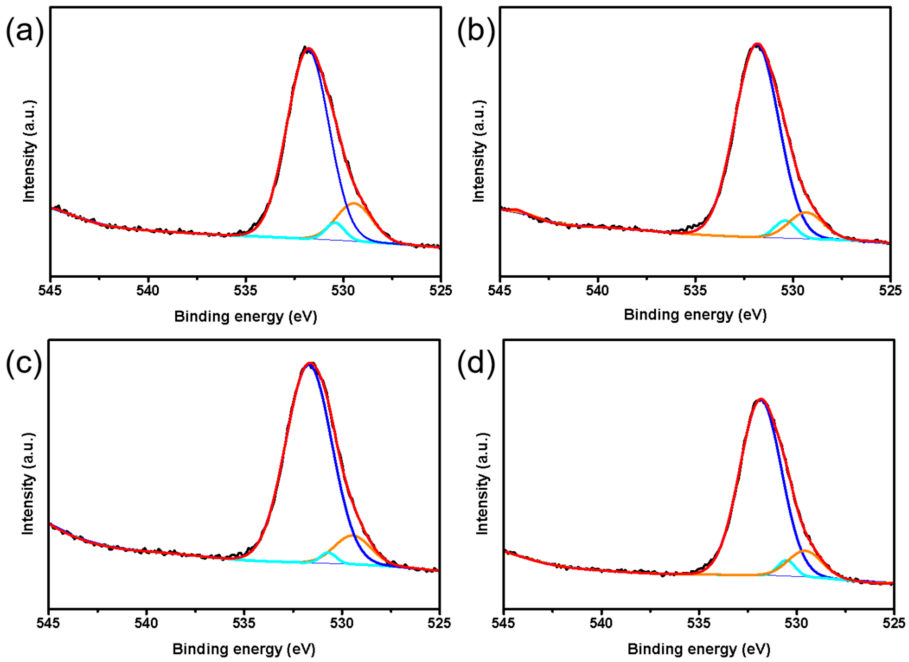


**Figure 10.** O 1s XPS spectra of peeled ABF substrates with different deposition times: (**a**) 0 min; (**b**) 2 min; (**c**) 5 min; (**d**) 10 min.

Figure 11 shows the N 1s XPS spectra of the peeled ABF substrates with different PDA deposition times. The N 1s peaks of all the samples were fitted using Origin software version 9.0, and all the N 1s peaks were resolved into two sub-peaks. These sub-peaks are assigned to C=N (peak one) and C-NH-C/$NH_2$ (peak two) bonds, where the C=N and C-NH-C/$NH_2$ peaks primarily originate from the polymer chains of the ABF and PDA. Based on the fitted results (see Table S3), the integral areas of peak two are 78.77%, 94.92%, 92.87%, and 98.94%, respectively. This result shows that when the deposition time was increased from 0 to 10 min, the integral area of peak two increased significantly, indicating that almost all the newly added nitrogen species on the peeled surface originated from the amine structures in PDA. At the same time, the integral areas of peak two at 2 min and 10 min are higher than that at 5 min. This phenomenon is mainly attributed to the fact that more C-NH-C/$NH_2$ groups reacted with copper oxides to form chemical bonds. Consequently, when the copper strips were peeled, more of these active groups were transferred onto the surfaces of the copper strips, in comparison with the sample exhibiting lower adhesion strength.

Figure S2 shows the Cu LMM Auger spectra of the ABF substrates with different PDA deposition times. In general, there are two peaks in the Auger spectra at 568 eV and 570 eV, which correspond to peak one and peak two, respectively. However, herein, only one prominent characteristic peak was observed in all the samples at 568 eV, labeled as peak one. Notably, peak one (570 eV) corresponds to $Cu_2O$, whereas peak two (568 eV) corresponds to pure copper [25,26]. In order to further analyze the change trends of these two peaks, the Cu LMM spectra were resolved into two sub-peaks using Origin software version 9.0, and the fitted results are shown in Figure S3 and Table S4. As seen, the

integral area of peak one exhibits a very small change, indicating that the introduction of PDA can stabilize the interfacial oxidation behavior compared with the unmodified ABF/Cu interfaces.

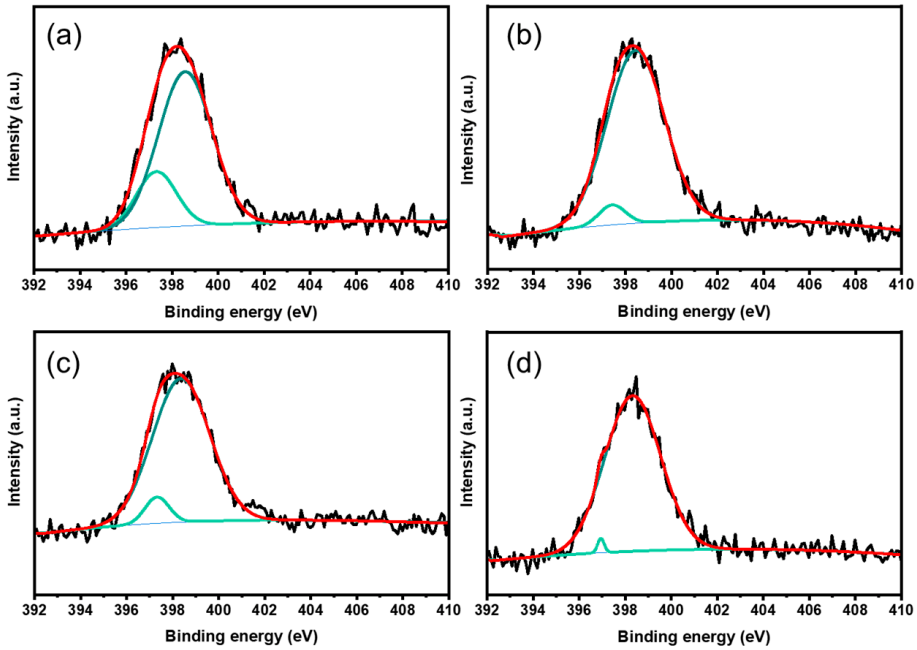


**Figure 11.** N 1s XPS spectra of peeled ABF substrates with different deposition times: (**a**) 0 min; (**b**) 2 min; (**c**) 5 min; (**d**) 10 min.

In order to evaluate the adhesion property between the copper and the ABF substrate, the 90° peel-off testing method was used to carry out peel experiments on the ABF substrates, as shown in Figure 12. Figure 12a shows the photograph of the ABF substrates with dimensions of 10 cm × 10 cm after annealing at 190 °C for 1 h. The ABF substrate was cut into 5 cm × 1 cm samples, and then the copper strips on the surface of the samples were peeled, as shown in the inset of Figure 12b. The peeling results of the ABF substrates with different PDA deposition times are shown in Figure 12b. As a result, the adhesion strength first increased from 2.2 N/cm to 4.1 N/cm, and then decreased to 3.2 N/cm when the deposition time was increased from 0 min to 10 min. These results are attributed to the following factors: (1) the density of polar groups on the surface of the desmeared ABF substrates increases. This is because PDA deposition can introduce polar functional groups such as amine, quinone, phenolic hydroxyl, and indole groups, that can form strong chemical and physical bonds with the fillers, copper, copper oxides, and the epoxy resin, which subsequently generate chemical covalent bonds such as C-O-Cu, C-N-Cu, and C=O-Cu, as shown in Figures S5 and S6; (2) the polar groups on the surface of the ABF regulate the content and composition of the copper oxides at the interfaces. This regulation leads to a decrease in the copper oxides, thereby reducing the weak phase layer in copper oxides and enhancing the interfacial strength; (3) when the thickness of the PDA layer becomes greater, the cohesive energy of the PDA layer is weaker than that of the ABF resin; consequently, the PDA layer will break down first, leading to a decrease in the adhesion strength when the deposition time reaches 10 min.

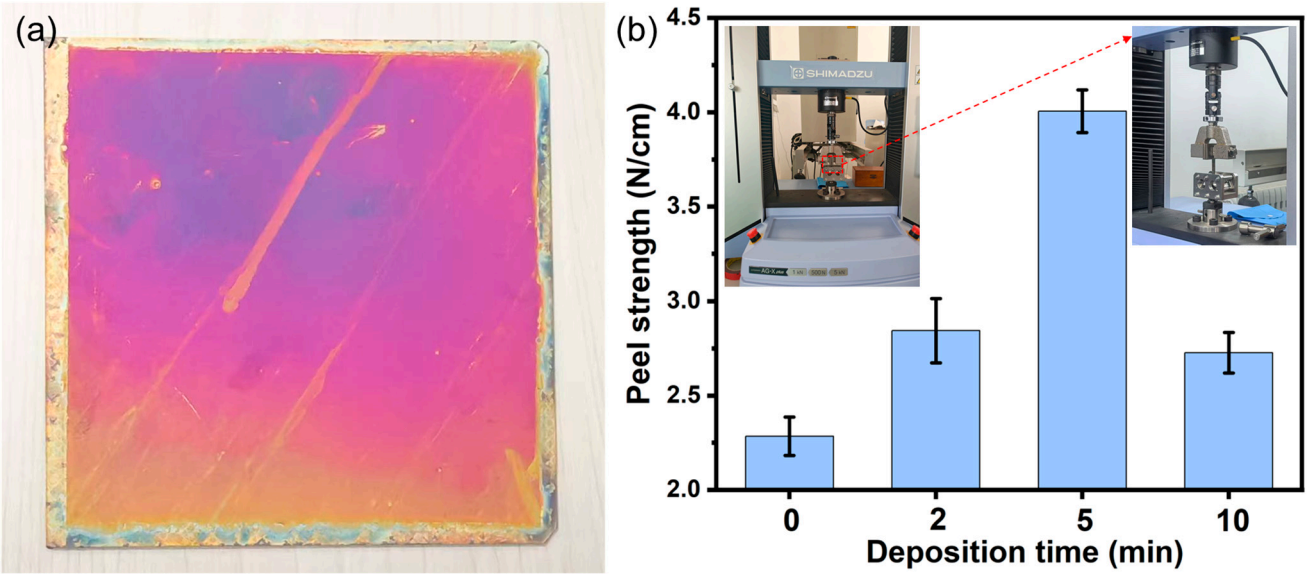


**Figure 12.** (**a**) Photo image after annealing; (**b**) peel strength of PDA@ABF samples with different deposition times of PDA.

## 4. Conclusions

In summary, PDA-modified ABF substrates with four layers were fabricated, and the effect of the PDA deposition time on the interfacial adhesion strength between the copper and the ABF substrate was systematically studied. The surface morphology, surface roughness, chemical states, and adhesion strength were characterized to analyze the evolution mechanism of the interfacial properties. The results showed that as the PDA deposition time increased, the adhesion strength first increased from 2.2 N/cm to 4.1 N/cm and then decreased to 3.2 N/cm; at the same time, the copper oxide content decreased from 14.05% to 9.96%. The adhesion strength and copper oxides were regulated by the polar groups on the surface of the PDA@ABF substrates. This is because the deposition of PDA not only can increase the interfacial chemical bonding action in comparison with pure ABF but also can tune the layer thickness of the copper oxides as a weak phase at the interfaces. This study elucidates the enhancement mechanisms of adhesion strength, providing valuable guidance for improving the interfacial adhesion properties of packaging substrates in future applications.

**Supplementary Materials:** The following supporting information can be downloaded at: https://www.mdpi.com/article/10.3390/chips5030023/s1, Figure S1: Polymerization mechanism of polydopamine.; Figure S2: XPS survey spectra of the peeled copper strip surfaces with different PDA deposition times.; Figure S3: Cu LMM AES spectra on the surface of peeled copper strips with different PDA deposition time.; Figure S4: Fitted Cu LMM AES spectra on the surface of peeled copper strips with different PDA deposition time: (a) 0 min; (b) 2 min; (c) 5 min; (d) 10 min.; Figure S5: Bonding mechanism between polydopamine and copper oxide.; Figure S6: Bonding mechanism between polydopamine and ABF; Table S1: The fitted integral area of C1s XPS spectra on the surface of peeled copper strips with PDA deposition times; Table S2: The fitted integral area of O1s XPS spectra on the surface of peeled copper strips with PDA deposition times. Table S3: The peak intensities of N1s XPS spectra on the surface of peeled copper strips with PDA deposition times.; Table S4: The fitted integral area of Cu LMM XPS spectra on the surface of peeled copper strips with different PDA deposition times.

**Author Contributions:** Conceptualization, S.D.; methodology, X.L.; software, X.L.; validation, M.L. (Mengxi Liu), M.L. (Man Li) and X.L.; formal analysis, Q.A.; investigation, C.C. and X.W.; resources, Z.F. and Q.W.; data curation, X.L. and M.L. (Mengxi Liu); writing—original draft preparation, S.D.;

writing—review and editing, S.D.; visualization, C.C. and X.W.; supervision, S.D. and Q.W.; project administration, S.D. and Z.F.; funding acquisition, S.D., M.L. (Man Li) and X.W. All authors have read and agreed to the published version of the manuscript.

**Funding:** This work was supported by the Beijing Natural Science Foundation (Grant No. 4254117) and Beijing Natural Science Foundation (Grant No. 4264148) and the Self-deployment Project of State Key Laboratory of Fabrication Technologies for Integrated Circuits.

**Informed Consent Statement:** Not applicable.

**Data Availability Statement:** Dataset available on request from the authors.

**Conflicts of Interest:** The authors declare no conflicts of interest.

## References

1. Nimbalkar, P.; Bhaskar, P.; Vijay Kumar, L.N.; Narayanan, M.; Torres, E.; Ambi Venkataramanan, S.S.; Kathaperumal, M. A review of glass substrate technologies. *Chips* **2025**, *4*, 37. [CrossRef]
2. Ding, S.J.; Zhao, J.Y.; Wu, X.M.; Chen, C.; Fang, Z.D.; Wang, Q.D. Curing kinetics of a novel commercial epoxy-phenolic composite build-up film for flip-chip ball grid array (FCBGA) substrates. *Microelectron. J.* **2025**, *161*, 106717. [CrossRef]
3. Ding, S.J.; Zhao, J.Y.; Wu, X.M.; Sun, P.; Yang, F.; Gui, M.Q.; Chen, C.; Fang, Z.D.; Wang, Q.D. Review on warpage mechanisms and control of packaging substrates for large-scale chiplet integration. *J. Mater. Sci. Mater. Electron.* **2025**, *36*, 2149. [CrossRef]
4. Zhang, K. TSMC 2025 Technology Symposium Press Briefing. Presented at the TSMC North America Technology Symposium, Santa Clara, CA, USA, 23 April 2025. Available online: https://semiwiki.com/semiconductor-manufacturers/tsmc/355121-tsmc-2025-technical-symposium-briefing/ (accessed on 14 June 2026).
5. Yu, J.Y.; Yang, Y.Q.; Liu, Y.C.; Li, W.D.; Xu, P.P.; Wang, Y.; Yu, S.H.; Luo, S.B. Construction Rivet Structure on Build-up Film with Low Surface Roughness and High Adhesion Strength for IC Packaging Substrates. *Surf. Interfaces* **2026**, *95*, 109671. [CrossRef]
6. Luo, S.B.; Sui, Y.Y.; Yu, J.Y.; Gao, C.B.; Zhu, C.X.; Xu, P.P.; Li, W.D.; Wei, X.; Yu, S.H. Scalable $SiO_2$/Epoxy Dielectric Films for High-Yield and Fine-Line Substrate Fabrication via Copper Tooth Transfer Printing. *Adv. Eng. Mater.* **2026**, *28*, e202502745.
7. Kempa, S.; Friz, W.; Gaul, F.; Habig, E.; Gregoriades, L.J. Investigation of a proactive glass filler removal in IC substrate build up films and its effect on topography and copper adhesion reliability. *Int. Microelectron. Assem. Pack. Soc.* **2018**, *2018*, 000634–000639. [CrossRef]
8. Murayama, T.; Sakuishi, T.; Morikawa, Y. Surface-modification technology by using Radical Shower Treatment (RST) process in submicron interposer for Fan-out packaging applications. In Proceedings of the 2019 International Conference on Electronics Packaging (ICEP), Niigata, Japan, 17–20 April 2019; pp. 246–250.
9. Ding, S.J.; Wu, X.M.; Chen, C.; Gui, M.Q.; Sun, P.; Yang, F.; Zhang, X.; Fang, Z.D.; Wang, Q.D. Enhanced adhesion strength of copper deposited epoxy composite films for chip substrates by tuning copper oxide and internal stress. *Appl. Surf. Sci.* **2025**, *684*, 161911. [CrossRef]
10. Wang, Y.; Ni, L.; Yang, F.; Gu, F.; Liang, K.; Marcus, K.; Wan, Y.; Chen, J.; Feng, Z. Facile preparation of a high-quality copper layer on epoxy resin via electroless plating for applications in electromagnetic interference shielding. *J. Mater. Chem. C* **2017**, *5*, 12769–12776. [CrossRef]
11. Zhu, M.; Gan, M.; Pan, J.; Tu, J.; Wang, X.; Gu, C. Polydopamine/silane composite coating on electrolytic copper foil as epoxy adhesion promoter and corrosion inhibitor. *J. Electron. Mater.* **2023**, *52*, 8160–8174. [CrossRef]
12. Chou, S.C.; Chung, W.A.; Fan, T.L.; Dordi, Y.; Koike, J.; Wu, P.W. Polydopamine and its composite film as an adhesion layer for Cu electroless deposition on $SiO_2$. *J. Electrochem. Soc.* **2020**, *167*, 042507. [CrossRef]
13. Schaubroeck, D.; Eeckhout, E.V.D.; Baets, J.D.; Dubruel, P.; Vaeck, L.V.; Calster, A.V. Surface modification of a photo-definable epoxy resin with polydopamine to improve adhesion with electroless deposited copper. *J. Adhe. Sci. Technol.* **2012**, *26*, 2301–2314. [CrossRef]
14. Krogsgaard, M.; Nue, V.; Birkedal, H. Mussel-inspired materials: Self-healing through coordination chemistry. *Chem. A Eur. J.* **2016**, *22*, 844–857.
15. Liu, H.; Feng, Z.; Wang, K.; Lian, J.; Chen, Y.; Yang, M.; Wang, Y. An accessible strategy for high-performance copper layer fabrication on polyphenylene oxide substrates via polydopamine functionalization and electroless deposition. *J. Mater. Sci. Mater. Electron.* **2022**, *33*, 13012–13022. [CrossRef]
16. Silva, C.; Simon, F.; Friedel, P.; Pötschke, P.; Zimmerer, C. Elucidating the chemistry behind the reduction of graphene oxide using a green approach with polydopamine. *Nanomaterials* **2019**, *9*, 902. [CrossRef] [PubMed]
17. Silva, E.; Guillot, J.; Grysan, P.; Lenoble, D.; Barborini, E.; Arl, D. Role of metal ion promoters in carbon nanotubes functionalization by polydopamine in the perspective of electroplated copper–carbon composites. *React. Chem. Eng.* **2026**, *11*, 334–345. [CrossRef]

18. Roberts, B.C.; Jones, A.R.; Ezekoye, O.A.; Ellison, C.J.; Webber, M.E. Development of kinetic parameters for polyurethane thermal degradation modeling featuring a bioinspired catecholic flame retardant. *Combust. Flame* **2017**, *177*, 184–192. [CrossRef]
19. Rocha, J.F.; de Oliveira, J.C.; Bettini, J.; Strauss, M.; Selmi, G.S.; Okazaki, A.K.; Oliveira, R.F.D.; Lima, R.S.; Santhiago, M. Tuning the chemical and electrochemical properties of paper-based carbon electrodes by pyrolysis of polydopamine. *ACS Meas. Sci. Au* **2024**, *4*, 188–200. [CrossRef] [PubMed]
20. Zhang, C.; Ou, Y.; Lei, W.X.; Wan, L.S.; Ji, J.; Xu, Z.K. $CuSO_4/H_2O_2$-induced rapid deposition of polydopamine coatings with high uniformity and enhanced stability. *Angew. Chem. Int. Ed.* **2016**, *55*, 3054–3057. [CrossRef] [PubMed]
21. Luo, S.B.; Yu, J.Y.; Ma, P.L.; Gao, C.B.; Li, P.; Zhu, C.; Yang, Y.Q.; Xu, P.P.; Yang, J.; Sun, R.; et al. Strong Adhesion of Electroless Plated Copper by Optimizing Lamination Temperature of Epoxy Composite Film for Advanced Chip Packaging Substrates. *Adv. Eng. Mater.* **2024**, *26*, 2400736. [CrossRef]
22. Ding, S.J.; Wu, X.M.; Zhang, X.; Gui, M.Q.; Fang, Z.D.; Wang, Q.D. Heterointerfacial adhesion failure mechanism of ultrahigh filler loading containing epoxy composite films for chip substrates. *RSC Appl. Interfaces* **2024**, *1*, 1214–1221. [CrossRef]
23. Eun, K.; Sung, K.J.; Kim, J.M.; Jang, S.H.; Yoon, S.; Lee, S.; Kim, W.; Han, S.; Son, H.Y.; Lee, K. Enhancement of the Adhesion in Multilayer Redistribution Layers of Fan-Out Wafer Level Package for Memory Applications. In Proceedings of the 2025 IEEE 75th Electronic Components and Technology Conference (ECTC), Dallas, TX, USA, 27–30 May 2025; pp. 522–525.
24. Ding, S.J.; Li, M.; Liu, M.X.; Wu, X.M.; Chen, C.; An, Q.C.; Fang, Z.D.; Wang, Q.D. Enhanced interfacial adhesion strength and reduced warpage of copper electrodeposited epoxy composite substrates by annealing treatment. *Surf. Interfaces* **2026**, *84*, 108573. [CrossRef]
25. Lee, H.J.; Yu, J. Study on the effects of copper oxide growth on the peel strength of copper/polyimide. *J. Electron. Mater.* **2008**, *37*, 1102–1110. [CrossRef]
26. Cho, K.; Cho, E.C.; Park, C.E. Effect of the physical and mechanical properties of epoxy resins on the adhesion behavior of epoxy/copper leadframe joints. *J. Adhes. Sci. Technol.* **2001**, *15*, 439–456. [CrossRef]


**Disclaimer/Publisher's Note:** The statements, opinions and data contained in all publications are solely those of the individual author(s) and contributor(s) and not of MDPI and/or the editor(s). MDPI and/or the editor(s) disclaim responsibility for any injury to people or property resulting from any ideas, methods, instructions or products referred to in the content.